



Development of a Disposable Infusion System for the Delivery of Protein Therapeutics

David T. Eddington¹ and David J. Beebe²

¹Division of Health Sciences and Technology, Harvard-MIT, 77 Massachusetts Ave., E19-582 Cambridge, MA 02139, USA

²Department of Biomedical Engineering, University of Wisconsin-Madison, 1550 Engineering Dr., Madison, WI 53706, USA

Abstract. This paper describes the development and optimization of a low flow open-loop infusion device for continuous delivery of protein therapeutics. Specifically, a non-electronic polymer device is actuated with responsive hydrogels to infuse at 2 $\mu\text{L/hr}$ for 12 hours. Hydrogel actuators transduce a chemical signal (change in pH of the local environment) into a mechanical response (swelling) generating the pressure to drive the infusion. The hydrogel actuators are separated from the drug reservoir by an elastomeric impermeable membrane. As the hydrogel actuators expand, the expansion deflects the flexible membrane down and reduces the volume of the drug reservoir causing the infusion of drug through the needle that is the only outlet for the reservoir.

Key Words. hydrogel, infusion, protein therapeutics, PDMS

Introduction

High-throughput sequencing, DNA microarrays, genetic characterization of diseases, and high-performance computing for biological discovery are accelerating the discovery and understanding of diseases. These advances lead to the development of new protein drugs providing motivation for developing improved delivery technologies (Wooley and Mathies, 1994; Parekh and Rohlf, 1997; Burns et al., 1998; Kopp et al., 1998; Ronai et al., 2001). Generally, protein drugs are advantageous over small molecule drugs due to their ability to block interactions between macromolecules and their less toxicity making them desirable candidates for new therapies (Weng and DeLisi, 2002). However, unmodified proteins cannot be ingested as the acidic nature of the GI tract denatures the proteins, nor inhaled or delivered transdermally due to the large size of most proteins. Instead, proteins are either injected subcutaneously or intramuscularly. To combat this problem several portable and implantable infusion pumps have been developed and are on the market. However the need for a programmed delivery profile (current infusion systems do not incorporate sensing capabilities) make these devices less than ideal. Consequently, a number of research and commercial efforts underway aim to develop improved protein delivery vehicles and alternative approaches for protein delivery (Kim et al., 1999; Lin and Pisano, 1999; Jung et al., 2000; Cao et al., 2001; Martin and Grove, 2001;

Gu et al., 2002). However, none propose a comprehensive non-electronic technology serving both open and closed-loop designs with practical response times. Intensive insulin therapy for treating insulin dependant diabetes mellitus (IDDM) has very tight control needs, therefore this will be used as a model drug/disease to aid design iterations. The same methodologies can be used to apply the device to other protein infusion therapies increasing the impact of the proposed delivery system.

Patients with IDDM stabilize blood glucose levels with multiple daily subcutaneous insulin injections delivered by either a syringe or a portable programmable insulin pump. Both these methods rely on the patient to perform routine finger stick blood glucose measurements to monitor how their bodies react to insulin under different activities and scenarios. Since uncontrolled blood glucose levels result in long term complications, patient compliance remains as the largest factor in successful insulin therapy. With the trend toward more protein based therapies with similar long-term patient compliance implications, the need for better delivery vehicles becomes increasingly important. This paper outlines the first step in realizing this goal with the development of an open-loop infusion system. The system described in this paper meets the specific need of constant overnight infusion of insulin. Currently, children suffering from diabetes have tremendous difficulty sleeping through the night due to hypoglycemic events, which causes overall discomfort in the early hours of the morning, such as cold sweats. These hypoglycemic events occur as a result from the peaking action of injected insulin. The development of an open-loop insulin infusion device, which continuously infuses overnight, would eliminate hypoglycemic events. The device could be transformed into a closed-loop insulin infusion system with the addition of a glucose responsive microvalve to the outlet of this system. Such a glucose responsive microvalve currently does not exist, however several groups are working on filling this need (Miyata et al., 1996; Gu and Siegl, 2001; Soppimath et al., 2002; Baldi et al., 2003). Another benefit of constant infusion is there is no pool of subcutaneous insulin. After a patient injects insulin

subcutaneously, the insulin remains in the tissue until the insulin is absorbed resulting in the possibility of overdosing insulin. Recently, the combined use of fast acting (Regular, Lispro, Novolin) and long acting (Lantus or Glargine) insulin enables slightly more freedom for the patient, however there is no way to remove the pool of insulin once it is injected.

The real power of this open-loop device lies in its adaptability. With minor modifications (such as membrane thickness, chamber dimensions, or hydrogel chemistry) this device could deliver pharmaceuticals that cannot be ingested, inhaled, or delivered transdermally (e.g. proteins). Some immediate foreseeable applications for the device would be the administration of protein hormones, anti-clotting agents, pain control medications, and drugs used to treat cancer. One alternate specific application for the device is for early delivery of octreotide in patients with variceal bleeding due to cirrhosis (Nidegger et al., 2003). A recent study has reported very early delivery (by first responders) of octreotide improves survival following a variceal bleeding event. Octreotide needs a very low infusion rate and is traditionally administered through an IV, however when variceal bleeding events occur the blood volume of the patient is low making IV access difficult. Since these situations usually occur in emergency scenarios, the open-loop device described in this paper presents a simpler method for delivery and may improve patient survival following a variceal bleeding event.

Background

Device design

The device consists of a micromolded polydimethylsiloxane (PDMS) fluidic network with pH responsive hydrogel actuators as shown in Figure 1. Responsive hydrogels are materials able to change volume in response to a stimulus from the local environment. The reversible ionization of end groups initiates an osmotic pressure gradient causing the volume expansion or contraction of the hydrogel via the movement of water into and out of the gel (Sudipto et al., 2002). The hydrogel actuators are separated from the drug reservoir by an impermeable membrane and the chamber housing the actuators is vented to atmosphere to allow the increase in volume of the top chamber (and consequential decrease in volume of the reservoir). As the hydrogel actuators expand, the expansion deflects the flexible membrane down and reduces the volume of the drug reservoir causing the infusion of drug through the outlet of the reservoir. Two chambers were used instead of one large chamber to reduce the size of the chambers and prevent the membrane from collapsing under the weight of the hydrogels. Recently, Su et al. (2002) demonstrated an osmotic infusion system capable of open-loop infusion with very low flow rates. This paper presents an alternate route to fluidic delivery with the potential to combine sensing and actuation within a single element (responsive hydrogel actuators), which is not possible with an osmotic infusion system.

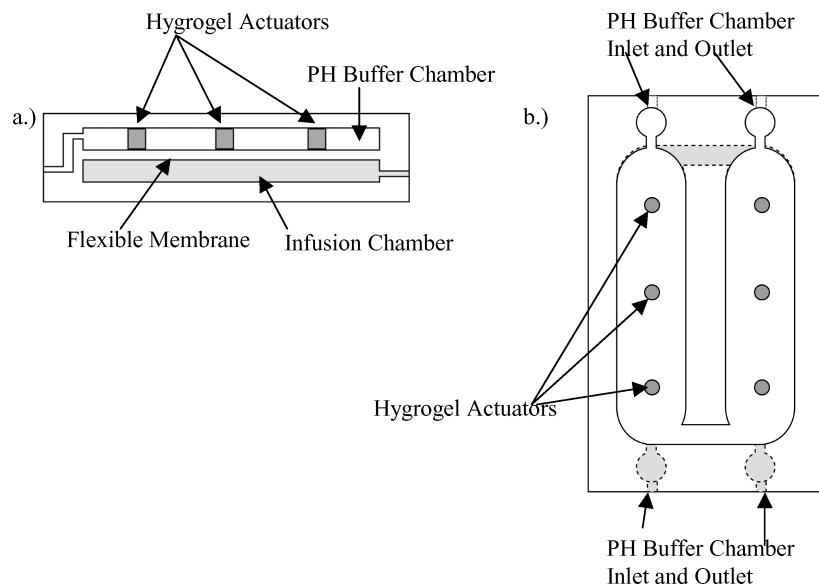


Fig. 1. Schematic showing (a) the side view and (b) top view of the device. The 6 hydrogel actuator posts are shaded grey.

Hydrogel actuators

Kuhn et al. first demonstrated volume transitions in hydrogels in 1950, realizing their potential by dubbing them 'chemical muscles' (Kuhn et al., 1950). More recently hydrogels have been found to control fluid transport in the xylem of plants (Zwieniecki et al., 2001a, 2001b). In ionic hydrogels, the reversible ionization of end groups initiates an osmotic pressure gradient causing the volume expansion or contraction of the hydrogel via the movement of water into and out of the gel (Amsden, 1998; De et al., 2002). By altering the chemistry of the hydrogel, different functionalities have been developed to respond to a wide variety of signals including pH (Tanaka et al., 1980), temperature (Hoffman et al., 1999), light (Suzuki and Tanaka, 1990), glucose (Miyata et al., 1996; Kataoka et al., 1998; Jung et al., 2000; Guiseppi-Elie et al., 2002; Ogawa et al., 2002; Parmpi and Kofinas, 2004), antigens (Miyata et al., 1999), electric field (Basseti and Beebe, 2002) and magnetic field (Kato et al., 1997).

Hydrogel materials can be fabricated directly in devices through liquid photopolymerization (Beebe et al., 2000; Simms et al., 2005) or fabricated in a separate step and incorporated into the device (De et al., 2002). The liquid photopolymerization process involves a pre-polymer solution consisting of monomer, cross-linker and photo-initiator and patterned by initiating polymerization via UV radiation through a photo mask.

Methods

Fabrication of the device occurs in two distinct stages. First, the hydrogel actuators are photopolymerized using a stencil procedure as developed for mechanics experiments with hydroxyethylmethacrylate-co-acrylic acid (HEMA-AA) hydrogels (De et al., 2002). Due to the large size of the hydrogel actuators (3 mm diameter \times 1 mm height) and large volume of the actuation chamber (1 mL), photopolymerization after the fluidic network is fabricated is not desirable due to the large amount of prepolymer needed. The PDMS stencil is cast from a thick resist (SU-8, Microchem) mold master. The stencil is then filled with the liquid hydrogel prepolymer and exposed with 15 mW UV at 365 nm for 120 seconds. The hydrogels are then manually removed from the stencil and placed in methanol to extract any unpolymerized prepolymer as detailed in Figure 2.

Next the reservoir chamber and actuation chambers are cast with PDMS from SU-8 mold masters. The PDMS layers are separated from the mold and activated in an oxygen plasma and bonded together. The oxygen plasma

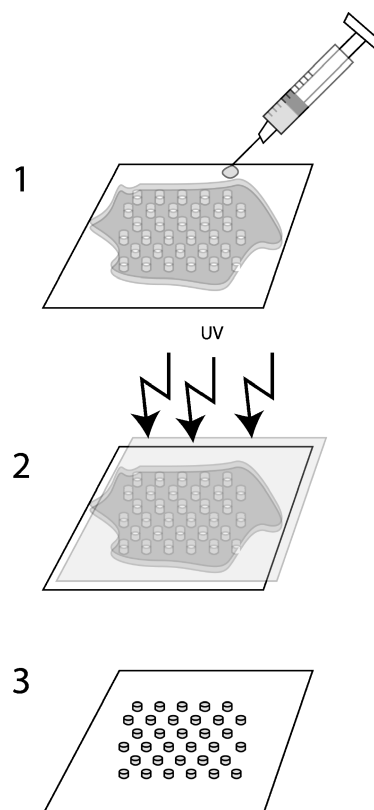


Fig. 2. Schematic showing hydrogel fabrication. (1) a PDMS stencil is placed on a sheet of PDMS and filled with liquid prepolymer. (2) A transparency is placed on top of the filled PDMS stencil and exposed to UV. (3) The stencil is peeled away and freestanding polymerized hydrogels remain.

breaks the bonds of the polymer backbone and forms reactive sites, which can recombine to form an irreversible bond when placed in conformal contact with another activated surface. The hydrogel actuators are integrated by manually placing them in the device between bonding steps. The 30 μ m PDMS membrane is fabricated by spin-casting PDMS onto a silicon wafer at 3500 rpm for 30 seconds.

The flowrate is measured by monitoring fluid flow through an outlet infusion line. The diameter of the outlet line is known and therefore the volume can be calculated with respect to time. The resistance of the outlet line is not enough to alter the flowrate (data not shown) due to the low flowrate. Data points are collected every 15 min throughout the experiment. The infusion is initiated through the addition of the phosphate buffer into the chamber containing the hydrogels followed by filling the drug reservoir to ensure injection of the triggering buffer does not affect the flowrate measurements.

Results and Discussion

Various parameters were investigated during the optimization process of the device including pH of the triggering buffer, PDMS membrane compliance, initial loading conditions on the actuator and morphology of the hydrogel actuators. The expansion profiles of hydrogels are known to be nonlinear, however through adjusting of various system parameters, a linear flow rate can be generated from a non-linear expansion profile. In this paper, the flow rate was measured and not the expansion rate of the hydrogel since the flow rate is the important device parameter. The optimization of the device can be separated into two efforts. First the PDMS microfluidic network was optimized for 6 hydrogel posts to ensure the dimensions of the chambers, including membrane thickness and chamber heights would maximize pumped volume for the specified time. Next the conditions of the hydrogel actuators were optimized including buffers used, loading conditions, and hydrogel morphology to achieve a linear flowrate.

Previous experiments determined the maximum force a hydrogel (600 μm diameter, 300 μm tall) produces during swelling to be 0.14 N (Johnson et al., 2004), corresponding to a stress of 0.5 MPa. This stress would strain a flexible membrane with a Young’s modulus of 1.0 MPa 55%. However, PDMS is an elastomer and hence does not have a linear stress strain curve above 10% strain. Therefore, the device should be designed to strain below 10% to ensure the linear relationship between stress and strain holds and proper design iterations can be made. A 12 mm wide actuation chamber ensures the membrane will not impede the volume expansion of the hydrogel (at full expansion, the maximum strain would be 2.6% as shown in Figure 3(a)). If the chamber width was narrower, it may approach the limit of force the hydrogel can exert

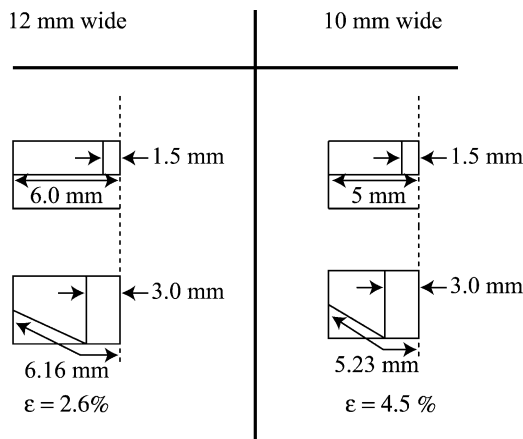


Fig. 3. Schematic showing a cross section of the device and how two chamber widths affect the membrane strain (ϵ).

and diverge from the linear range of stress and strain. The goal of constant infusion would make this divergence unfavorable. Generally, the width of the chamber is the most important device parameter to maximize the deflection of the membrane. By changing the width of the chamber by 3 mm, the strain in the membrane nearly doubles as shown in Figure 3(b), which may prove a direct route to tuning the infusion rate of the device as long as it stays below 10% strain.

Previous devices with hydrogel actuators (pH regulation system (Eddington et al., 2001; Eddington and Beebe, 2004)) utilized a pH 12 buffer since these generated the fastest response times from the hydrogel, which was advantageous for feedback controlled schemes. However in this device, longer times are ideal to ensure expansion over the specified time window. Earlier experiments performed also correlate a more linear expansion with a buffer with lower pH (Bauer, 2002). In our experiments, introducing a pH 8 phosphate buffer produced a similar flow profile when compared to a pH 12 phosphate buffer as shown in Figure 4. The device with the lower pH buffer did indeed expand over a longer period of time, but the volume expansion rate was still non-linear. However, the pH 8 buffer is advantageous since it poses less of a risk if there is an accidental release of buffer since the device will be worn on the skin. While changing the pH of the buffer did not solve the constant expansion issue, it did provide a safer means for triggering the hydrogel and also increased the time the hydrogels expanded. Therefore, further device iterations will employ the pH 8 buffer to trigger the hydrogels as opposed to the pH 12 buffer.

It was then postulated that perhaps the hydrogel actuators were initially expanding with no resistance from

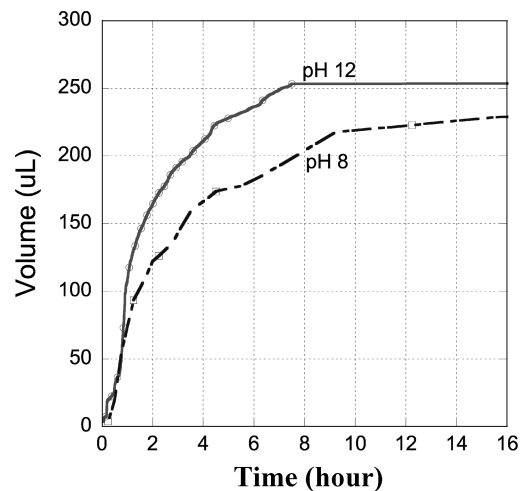


Fig. 4. Plot showing the infused volume with respect to time for a device triggered by pH12 and pH8 0.1 M phosphate buffer.

the PDMS membrane, but then reached an increasing resistance to deformation and were not able to expand as fast. Earlier experiments showed the hydrogel was able to produce a force of 0.14 N, correlating to a stress of 0.5 MPa for a 600 μm diameter hydrogel post. However the hydrogel posts used in the current device were four times as large. A larger hydrogel (3000 μm diameter, 1000 μm height) may not produce the same force as a smaller hydrogel (600 μm diameter, 200 μm height) rendering previous strain calculations inaccurate.

Therefore, the flow rate was studied as a function of membrane compliance. Three different devices were tested with membranes having different compliances. The compliance was modified through altering the ratio of prepolymer to hardener during PDMS preparation. Ratios (prepolymer to hardener) of 7:1, 11:1, and 15:1 were chosen to create a device with a stiffer membrane (7:1) a normal stiffness membrane (11:1) and a more compliant membrane (15:1). If the stiffness of the membrane affected the flow rate, the flow rate profiles would shift left for stiffer membranes and right for more compliant membranes since stiffer membranes would reach the maximum strain earlier than more compliant membranes. The results did not show any of these correlations as presented in Figure 5 which validated our initial calculations.

While it is known that an unconstrained hydrogel expands in an isotropic manner, it was unknown how a constrained hydrogel expanded. If the constrained hydrogel was not isotropic, the expansion in the z direction may differ from the x and y direction. This non-isotropic expansion would create a non-linear flow rate. To test this,

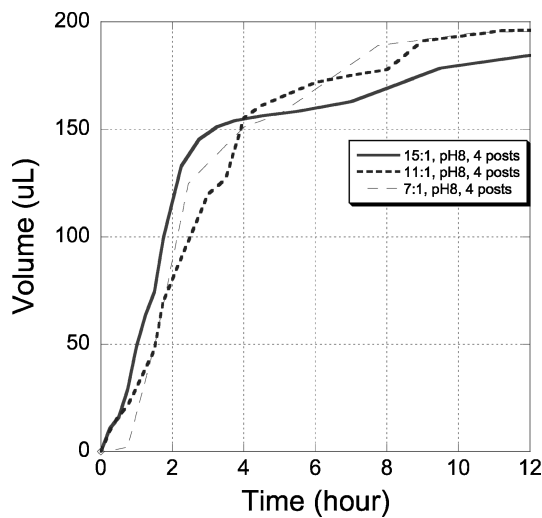


Fig. 5. Plots of devices with a 7:1 membrane, 11:1 membrane and 15:1 membrane and how it affected the flow rate. As shown by the figure all the infusion profiles were approximately equal.

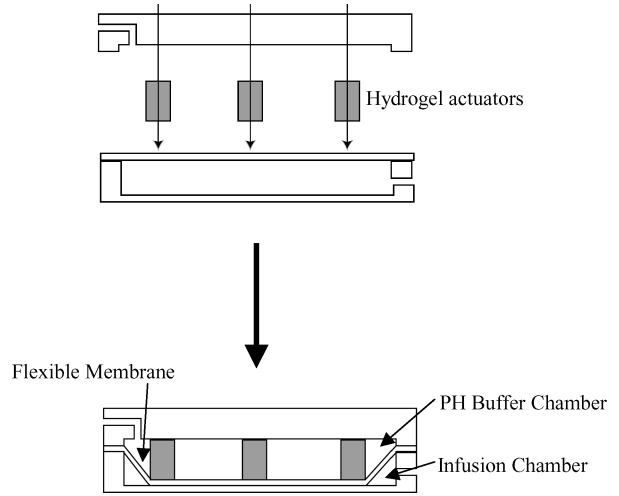


Fig. 6. Side view of how the prestrained device is fabricated.

a new device was fabricated to eliminate any expansion in the z direction by reducing the height of the actuation chamber so when the hydrogel is incorporated, the hydrogel initially stretches the membrane as shown by Figure 6, which we will refer to as prestrained. It was postulated that the constrained expansion in the x and y directions would produce a linear flow rate profile if the z -direction expansion was non-linear and the x and y expansion was linear. The results show the infusion profile is similar for the unconstrained device as for the prestrained device as shown in Figure 7. Another interesting aspect to this experiment is the overall shape of the volume expansion is unchanged when comparing the prestrained device to the unconstrained device with the two scenarios plotted on the same time axis as shown in Figure 7(b). This leads to the conclusion the hydrogel posts expand the same in all directions regardless of loading conditions.

The membrane compliance and preloading conditions have been ruled out as causes for the non linear volume expansion. The only remaining conclusion is hydrogel posts follow this typical infusion profile regardless of external conditions on the hydrogel. Therefore, only changing the geometry of the hydrogel will change the shape of the infusion profile. Changing the shape will change how the hydrogel is able to expand. If the area exposed to triggering buffer with respect to time is more constant, a more uniform expansion profile would be generated. If a circle is divided into three regions with a thickness of x as shown in Figure 8, the outer ring has an 80% larger cross sectional area than the inner ring. However a rectangle's outer and inner ring differ by only 20% as shown in Figure 8. Therefore, a rectangular hydrogel was incorporated into the system in an attempt to achieve a constant flowrate (30 mm length, 3 mm width, 1 mm height). The infusion

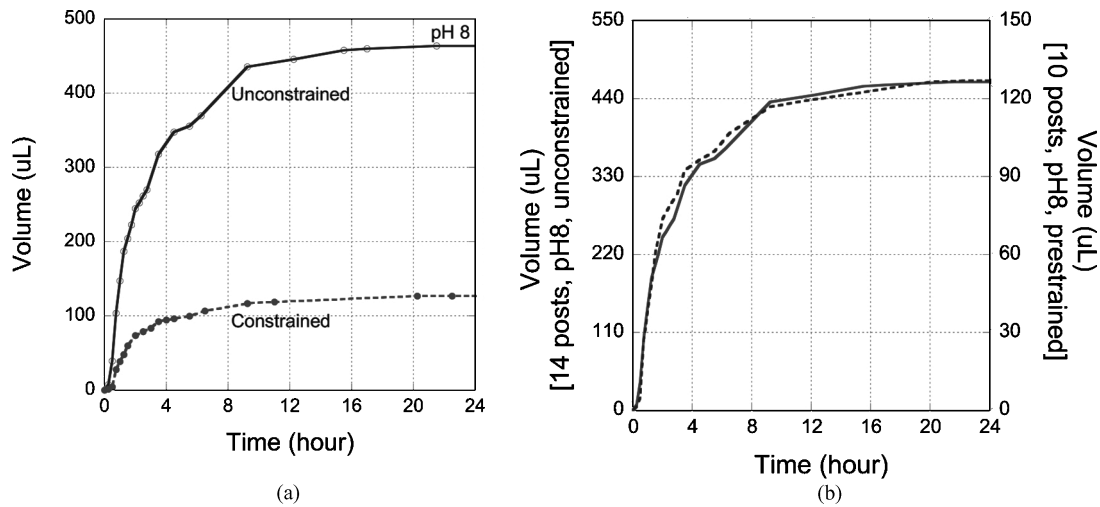


Fig. 7. (a) Plot showing the infusion profiles for an unconstrained device with 14 posts compared to a prestrained device with 10 posts. (b) Plot showing infusion profiles on separate y axis to illustrate similarities between devices.

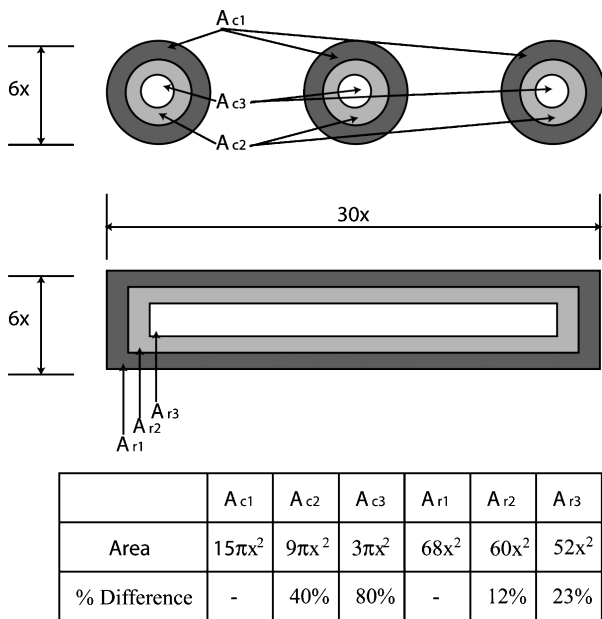


Fig. 8. Schematic illustrating the volume difference with concentric circles and rectangles. If a rectangle is used, the change in areas is less variable than with circles.

profile for the rectangular hydrogel is shown in Figure 9 as compared to a hydrogel post.

The infusion profile for the rectangular hydrogel is approximately linear over the first twelve hours with an average flowrate of $2 \mu\text{L/hr}$. This infusion rate is approximately five times slower than necessary for insulin therapy using U100 insulin, which has 100 units of insulin dissolved in 1 mL of aqueous solution (water, protamine sulfate, glycerin, m-cresol, methylparaben, phenol, and

zinc) and each unit of insulin has 0.04 mg of insulin protein. However U500 could be used which is a form of insulin five times more concentrated than normal U100 insulin. U500 insulin is not widely used, but is available through EliLilly. Therefore, a device using U500 insulin would need to infuse at $2 \mu\text{L/hr}$. The U500 insulin would potentially aggregate more than U100 insulin, however the pressure of the hydrogel should be enough to overcome this potential obstacle since the device was shown to dispense against a pressure head of 20 kN/m^2 , which would be enough to overcome blockages resulting from aggregation of insulin. In addition the outlet for the device could be routed through an array of microneedles. The clogging of one microneedle would not stop the outlet flow rate since there would be multiple paths. Several groups have developed microneedles for such an application (Lin and Pisano, 1999; Zahn et al., 2000; Griss and Stemme, 2002).

The experiment with the two rectangular hydrogels was run five times using a different device each time to validate the design. The results from this experiment are shown in Figure 10 and the flowrates range from $2.5 \mu\text{L/hr}$ to $1.0 \mu\text{L/hr}$. The hydrogels were stored in a pH 2 buffer solution before they were incorporated into the device, which most likely resulted in some hydrolysis of the crosslinks. This hydrolysis caused the hydrogel to expand more since there was less crosslinks in the hydrogel network. This coincides with the flowrates since the devices with the youngest hydrogels resulted in a $1.0 \mu\text{L/hr}$ infusion rate and the infusion rate increases with age of the hydrogels and hydrolysis of the crosslinks. Therefore, if the fabrication process is more closely regulated, such as storage conditions of the hydrogel actuators, it would be possible to fabricate a device with a repeatable infusion rate.

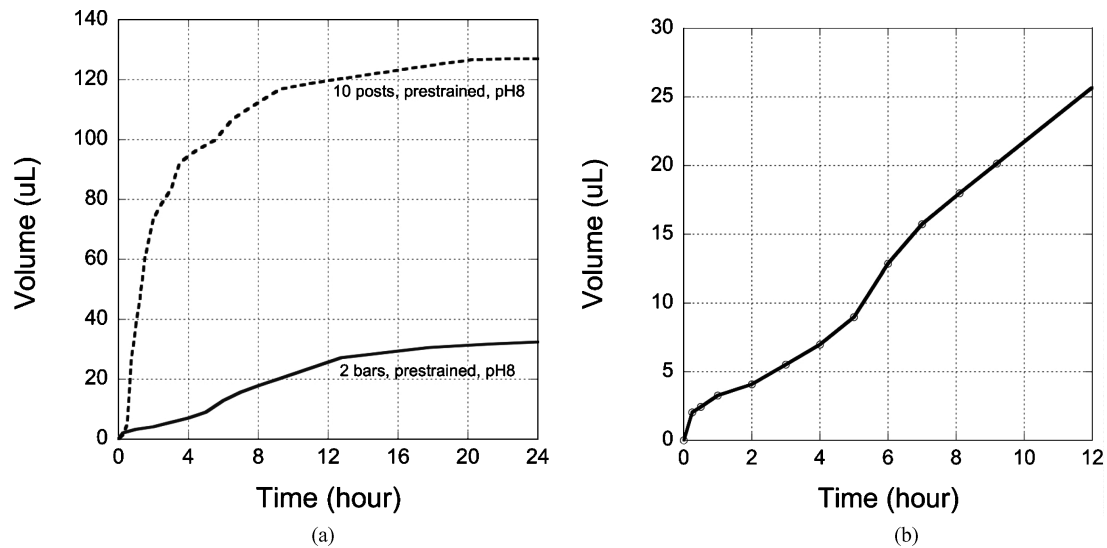


Fig. 9. (a) Infusion profile of a rectangular bar and a hydrogel post. (b) Expanded view of the infusion profile for the two bars.

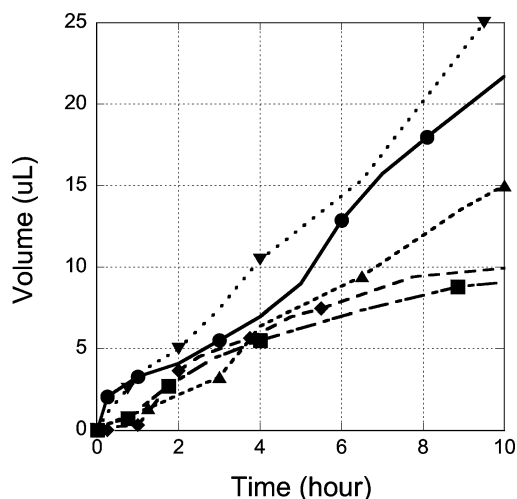


Fig. 10. Plot showing the infusion profile with respect to time for five devices with two hydrogel bars.

In addition the hydrolysis of the hydrogel actuators can be controlled to tune the device for a specific application. However, further experiments would be needed to quantify this phenomenon.

Conclusion

Using hydrogels as actuators in infusion systems eliminates the need for complicated electronics and control. This paper details the development of an external open-loop infusion system. The device demonstrated near linear flow over 12 h at $2.0 \mu\text{L/hr}$. The device will be further validated on an animal model in future experiments. The linear

flowrates achieved with the rectangular hydrogel bar arise from the geometry of the hydrogel. The rectangular hydrogels have a more uniform cross sectional area exposed to the triggering buffer with time, which results in a more uniform expansion profile.

References

- B. Amsden, *Macromolecules* **31**, 8382–8395 (1998).
- A. Baldi, Y. Gu, P.E. Loftness, R.A. Siegel and B. Ziaie, *Journal of Microelectromechanical Systems* **12**, 613–621 (2003).
- M.J. Bassetti and D.J. Beebe, *Micro Total Analysis Systems 2002*, Kluwer Academic Publishers (Nara, Japan, 2002).
- J.M. Bauer, Fabrication and analysis of microscale hydrogels and polymers. Urbana, University of Illinois at Urbana-Champaign **163**, (2002).
- D.J. Beebe, J.S. Moore, J.M. Bauer, Q. Yu, R.H. Liu, C. Devadoss, and B.H. Jo, *Nature* **404**, 588–590 (2000).
- M. Burns, B. Johnson, S. Brahmasandra, K. Handique, J. Webster, M. Krishnan, T. Sammarco, P. Man, D. Jones, D. Heldsinger, C. Mastrangelo, and D. Burke, *Science* **282**, 484–487 (1998).
- X. Cao, S. Lai, and L.J. Lee, *Biomedical Microdevices* **3**, 109–118 (2001).
- S.K. De, N.R. Aluru, B. Johnson, W.C. Crone, D.J. Beebe, and J. Moore, *Journal of Microelectromechanical Systems* **11**, 544–555 (2002).
- D.T. Eddington and D.J. Beebe, *Journal of Microelectromechanical Systems* **13**, 586–593 (2004).
- D.T. Eddington, R.H. Liu, D.J. Beebe, and J.S. Moore, *Lab on a Chip* **1**, 96–99 (2001).
- P. Griss and G. Stemme, *Micro Electro Mechanical Systems*, IEEE (Piscataway, NJ, 2002).
- Y. Gu, A. Baldi, B. Ziaie, and R.A. Siegel, 2nd International IEEE-EMBS Special Topic Conference on Microtechnologies in Medicine and Biology, Madison, WI USA, IEEE (2002).
- Y.D. Gu and R.A. Siegel, *International Symposium on Controlled Release Bioactive Materials* (2001).
- A. Guiseppi-Elie, S.I. Brahim, and D. Narinesingh, *Advanced Materials* **14**, 743–746 (2002).

- J. Hoffman, M. Plotner, D. Kuckling, and W. Fischer, *Sensors and Actuators B* **77**, 139–144 (1999).
- B. Johnson, J.M. Bauer, D.J. Niedermaier, W.C. Crone, and D.J. Beebe, *Experimental Mechanics* **44**, 21–28 (2004).
- D.Y. Jung, J.J. Magda, and I.S. Han, *Macromolecules* **33**, 3332–3336 (2000).
- K. Kataoka, H. Miyazaki, M. Bunya, T. Okano, and Y. Sakurai, *Journal of the American Chemical Society* **120**, 12694–12695 (1998).
- N. Kato, F. Takahashi, and S. Yamanobe, *Material Science and Engineering C: Biomimetic Materials, Sensors and Systems* **C5**, 141–147 (1997).
- H.C. Kim, Y.H. Bae, and S.W. Kim, *IEEE Transactions on Biomedical Engineering*, **46**, 663–669 (1999).
- M.U. Kopp, A.J. deMello, and A. Manz, *Science* **280**, 1046–1049 (1998).
- W. Kuhn, B. Hargitay, A. Katchalsky, and H. Eisenberg, *Nature* **165**, 514–516 (1950).
- L. Lin and A.P. Pisano, *Journal of Microelectromechanical Systems* **8**, 78–84 (1999).
- F.J. Martin and C. Grove, *Biomedical Microdevices* **3**, 97–108 (2001).
- T. Miyata, N. Asami, and T. Uragami, *Nature* **399**, 766–796 (1999).
- T. Miyata, A. Jikihara, and K. Nakamae, *Macromolecular Chemistry and Physics* **197**, 1135–1146 (1996).
- D. Nidegger, S. Ragot, P. Berthelemy, C. Masliah, C. Pilette, T. Martin, A. Bianchi, T. Paupard, C. Silvain, and M. Beauchant, *Journal of Hepatology* **39**, 509–514 (2003).
- K. Ogawa, T. Nakajima-Kambe, T. Nakahara, and E. Kokufuta, *Biomacromolecules* **3**, 625–631 (2002).
- R.B. Parekh and C. Rohlff, *Current Opinion in Biotechnology* **8**, 719–723 (1997).
- P. Parmpi and P. Kofinas, *Biomaterials* **25**, 1969–1973 (2004).
- Z. Ronai, C. Barta, M. Sasvari-Szekely, and A. Guttman, *Electrophoresis* **22**, 294–299 (2001).
- H.M. Simms, C.M. Brotherton, B.T. Good, R.H. Davis, K.S. Anseth, and C.N. Bowman, *Lab on a Chip* **5**, 151–157 (2005).
- K.S. Soppimath, T.M. Aminabhavi, A.M. Dave, S.G. Kumbar, and W.E. Rudzinski, *Drug Development and Industrial Pharmacy* **28**, 957–974 (2002).
- Y.C. Su, L.W. Lin, and A.P. Pisano, *Journal of Microelectromechanical Systems*, **11**, 736–742 (2002).
- K.D. Sudipto, N.R. Aluru, B. Johnson, W.C. Crone, D.J. Beebe and J.S. Moore, *Journal of Microelectromechanical Systems* **11**, 544–555 (2002).
- A. Suzuki and T. Tanaka, *Nature* **346**, 345–347 (1990).
- T. Tanaka, D. Fillmore, S. Sun, I. Nishio, G. Swislow, and A. Shah, *Physical Review Letters* **45**, 1636–1639 (1980).
- Z. Weng and C. DeLisi, *Trends in Biotechnology* **20**, 29–35 (2002).
- A.T. Woolley and R.A. Mathies, *Proceedings of the National Academy of Science* **1994**, 11348–11352 (1994).
- J.D. Zahn, N.H. Talbot, D. Liepmann, and A.P. Pisano, *Biomedical Microdevices* **2**, 295–303 (2000).
- M.A. Zwieniecki, P.J. Melcher, and N.M. Holbrook, *Journal of Experimental Botany* **52**, 257–264 (2001a).
- M.A. Zwieniecki, P.J. Melcher, and N.M. Holbrook, *Science* **291**, 1059–1062 (2001b).